

## Misaligned magnetized accretion flows onto spinning black holes: magneto-spin alignment, outflow power and intermittent jets

KOUSHIK CHATTERJEE <sup>1,2</sup> MATTHEW LISKA <sup>3,4</sup> ALEXANDER TCHEKHOVSKOY <sup>5</sup> AND SERA MARKOFF <sup>6,7</sup>

<sup>1</sup>*Black Hole Initiative at Harvard University, 20 Garden Street, Cambridge, MA 02138, USA*

<sup>2</sup>*Harvard-Smithsonian Center for Astrophysics, 60 Garden Street, Cambridge, MA 02138, USA*

<sup>3</sup>*Center for Relativistic Astrophysics, Georgia Institute of Technology, Howey Physics Bldg, 837 State St NW, Atlanta, GA 30332, USA*

<sup>4</sup>*Institute for Theory and Computation, Harvard University, 60 Garden Street, Cambridge, MA 02138, USA*

<sup>5</sup>*Center for Interdisciplinary Exploration & Research in Astrophysics (CIERA), Physics & Astronomy, Northwestern University, Evanston, IL 60202, USA*

<sup>6</sup>*Anton Pannekoek Institute for Astronomy, University of Amsterdam, Science Park 904, 1098 XH Amsterdam, The Netherlands*

<sup>7</sup>*Gravitation Astroparticle Physics Amsterdam (GRAPPA) Institute, University of Amsterdam, Science Park 904, 1098 XH Amsterdam, The Netherlands*

### ABSTRACT

Magnetic fields regulate black hole (BH) accretion, governing both the inflow and outflow dynamics. When a BH becomes saturated with large-scale vertical magnetic flux, it enters a magnetically-arrested disk (MAD) state. The dynamically-important BH magnetic flux powers highly efficient relativistic outflows (or jets) and sporadically erupts from the BH into the disk midplane. Here we explore the evolution of MADs when the BH and gas angular momentum are misaligned, which is expected to be more common. Using numerical simulations, we find that jets from rapidly spinning, prograde BHs force the inner accretion flow into alignment with the BH spin via the magneto-spin alignment mechanism for disks initially misaligned at  $\mathcal{T} \lesssim 60^\circ$ . Extremely misaligned MAD disks, on the other hand, exhibit intermittent jets that blow out parts of the disk to  $\approx 100$  gravitational radii before collapsing, leaving behind hot cavities and magnetized filaments. These intermittent jet mechanism forms a mini-feedback cycle and could explain some cases of X-ray and radio quasi-periodic eruptions observed in dim AGN. Further, we find that (i) for BHs with low power jets, the BH spin and initial disk tilt angle changes the amount of horizon magnetic flux, and (ii) geometrically-thick, misaligned accretion flows do not undergo sustained Lense-Thirring (LT) precession. Thereby, we suggest that low-luminosity accreting BHs ( $\dot{M} \ll 10^{-3} \dot{M}_{\text{Edd}}$ ) are not likely to exhibit quasi-periodic oscillations in lightcurves due to LT precession, in agreement with observations of BH X-ray binaries and AGN in the low-hard/quiescent state. Instead, we suggest that magnetic flux eruptions can mimic precession-like motion, such as observed in the M87 jet, by driving large-scale surface waves in the jets.

*Keywords:* black hole physics - accretion - general relativity

### 1. INTRODUCTION

Outflowing collimated streams of magnetized plasma moving at relativistic speeds, called jets, are ubiquitously observed around compact objects, like black holes (BHs) and neutron stars. Owing to the enormous energy they carry, jets deposit their mechanical energy as they travel outward from the BH and can significantly heat

up interstellar medium (ISM) gas on interaction, forming a crucial component of the BH-galaxy feedback cycle (e.g., Fabian 2012; Harrison et al. 2018; Chatterjee et al. 2019). Further, jets could facilitate high energy particle acceleration via shocks or magnetic reconnection, and provide a viable origin for cosmic rays (e.g., Caprioli 2015; Sironi et al. 2015; Matthews et al. 2018; Crumley et al. 2019; Blandford et al. 2019).

Currently, the most plausible explanation for the high energy content of jets comes from the Blandford & Znajek (1977, hereafter BZ) mechanism where BH inertial

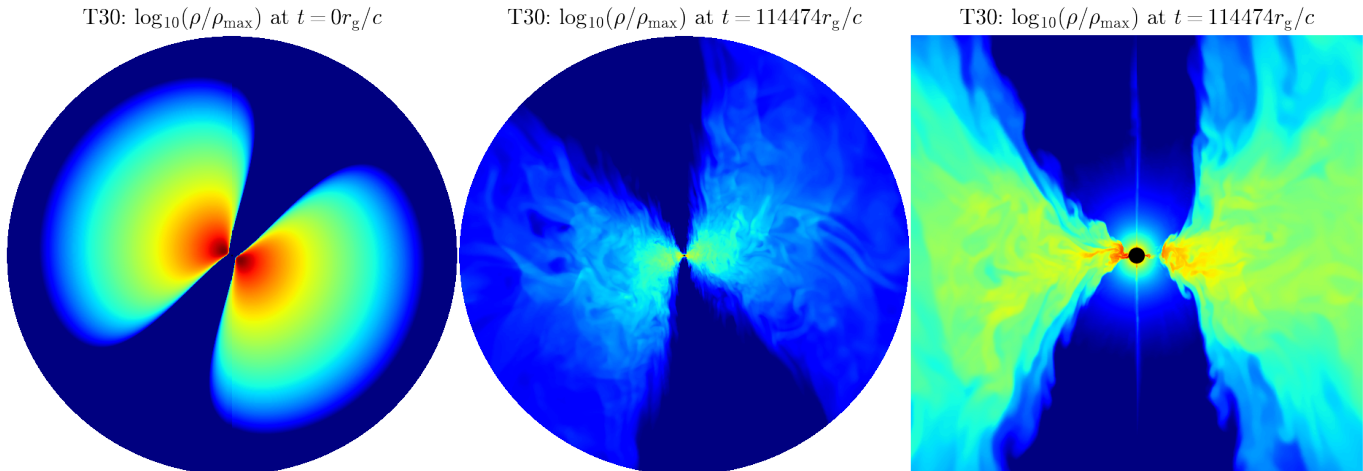


**Figure 1.** Initial and final states of a magneto-spin aligned accretion flow. We show vertical cross-sections of the gas density ( $\rho$ ) for a disk initially misaligned at  $30^\circ$  with respect to the black hole spin axis at time  $t = 0r_g/c$  (left panel) and at late times (middle and right panel). The left and middle panels show the full simulation grid, out to  $1000r_g$  while the right panel zooms in to the inner  $80r_g \times 80r_g$  of the grid. The color bar shows 5 orders of magnitude in density.

frame-dragging forces magnetized gas to corotate with the BH spin. This results in azimuthal twisting of vertical fields that produces an outward vertical pressure gradient and propels gas into a collimated outflow, forming jets. The BZ jet power depends on both the magnetic fields supplied to the BH as well as the BH spin  $a$ , and is given as  $P_{\text{BZ}} = (k\phi_{\text{BH}}^2\Omega_{\text{H}}^2)\dot{M}c^2$  (also see McKinney & Gammie 2004; Tchekhovskoy et al. 2010), where  $\phi_{\text{BH}}$ ,  $\Omega_{\text{H}} (= a/2r_{\text{H}})$  and  $\dot{M}$  are the dimensionless magnetic flux at the BH event horizon ( $r = r_{\text{H}}$ ), horizon angular frequency and mass accretion rate. The proportionality constant  $k$  depends on the shape of the magnetic field lines threading the horizon (e.g., Tchekhovskoy et al. 2010).

The BH spin dependence is particularly interesting as the maximum possible  $\phi_{\text{BH}}$  varies not only with the spin magnitude but also the direction, i.e., prograde or retrograde spin with respect to the accreting gas (Tchekhovskoy et al. 2012; Tchekhovskoy 2015; Narayan et al. 2022). Spin values are notoriously difficult to measure due to the turbulent nature of the accretion flow in the case of single BHs and the uncertainty in progenitor spins for equal-mass binary BH mergers. While current spin measurements for stellar mass BHs cluster around high values (for a review, see Reynolds 2021), there is evidence that galaxy mergers may result in small spins (Volonteri et al. 2005).

In regards to  $\phi_{\text{BH}}$ , the BH would be fed by the ISM that usually has approximately equipartition magnetic fields ( $\beta \sim 1$ ; Haverkorn & Spangler 2013; Ferrière 2020) due to galactic dynamos (e.g., Beck et al. 1996; Brandenburg & Subramanian 2005). Assuming a nominal

value of  $\sim \mu\text{Gauss}$ , one could argue that sufficient magnetic flux is available to saturate the BH magnetosphere (Narayan et al. 2003). Indeed, recent studies suggest that dynamically-strong magnetic fields may regulate the accretion of gas onto supermassive black holes (BHs) in low-luminosity active galactic nuclei (AGN), such as Sagittarius A\* (Sgr A\*) and M87 (e.g., Event Horizon Telescope Collaboration et al. 2019, 2022). The end state of magnetic-saturation, known as the magnetically arrested disk (MAD), produces highly efficient jets, which carry away angular momentum large enough to cause BH spindown (Tchekhovskoy et al. 2012; Narayan et al. 2022), especially for near- and super-Eddington BHs (Lowell et al. 2023; Ricarte et al. 2023). However, for the sub-Eddington accretion regime, conditions for the development of the MAD state and powerful jets appear optimal.

Usually, general relativistic magnetohydrodynamic (GRMHD) of accreting BHs assume that the rotation axis of the accretion disk and the BH spin are either aligned or anti-aligned. Allowing a tilt between the disk and the BH spin axes introduces interesting effects in the global disk structure such as radial tilt oscillations (Papaloizou & Lin 1995), Lense-Thirring (LT; Lense & Thirring 1918) precession, Bardeen-Petterson alignment (BP; Bardeen & Petterson 1975) and disk tearing (e.g., Nixon et al. 2012; Liska et al. 2021). Indeed, due to these additional effects, misaligned disks have been used to study quasi-periodic oscillations (QPOs) in lightcurves (see (for a review, see Ingram & Motta 2019) as well as near-horizon images of Sgr A\* and M87 (Dexter & Fragile 2013; Chatterjee et al. 2020; White et al. 2020;

Event Horizon Telescope Collaboration et al. 2022) with recent observations from Cui et al. (2023) showing hints of periodicity in the M87 jet position angle.

Misaligned accretion onto the BH occurs via plunging streams of gas (Fragile et al. 2007), possibly driven by nozzle shocks (as seen in thin disks; Kaaz et al. 2023) in contrast to the near-axisymmetric accretion seen for aligned BH-disk systems. This effect hinders the advection of magnetic fields close to the BH, reducing the horizon magnetic flux (Chatterjee et al. 2020). However, when supplied with MAD-level magnetic flux, the resulting jets can become powerful enough to force the disk to align, an effect known as magneto-spin alignment (McKinney et al. 2013; Polko & McKinney 2017; Ressler et al. 2021). The conditions that lead to magneto-spin alignment are yet to be understood clearly, especially the relation between disk alignment, BH spin and jet power. Further, it is unknown whether disk alignment is an inevitable consequence of the MAD state, which carries significant implications for galaxy evolution.

In this work, we simulate a wide variety of misaligned disks targeting the MAD state using the GRMHD code H-AMR. In Sec. 2, we describe our numerical choices and the model setup. Sec. 3 is broken into 4 parts, namely moderately and extremely misaligned disk models, the magneto-spin alignment effect, and outflow powers for tilted disks. We discuss two observational implications of our results in Sec. 4, shocks via disk-jet interactions and BH jet precession for sub-Eddington accretion flows. We provide a summary of our findings in Sec. 5.

## 2. NUMERICAL METHOD & MODEL SETUP

We use the GPU-accelerated code H-AMR (Liska et al. 2022) that solves the GRMHD equations in a fixed Kerr spacetime. We use a uniform grid in logarithmic spherical polar Kerr-Schild coordinates  $(t, \log r, \theta, \varphi)$ . We adopt geometrical units, i.e.  $G = c = 1$  in which the gravitational radius,  $r_g = GM_{\text{BH}}/c^2$ , equals the BH mass,  $M_{\text{BH}}$ . Our simulations have an effective grid resolution of  $N_r \times N_\theta \times N_\varphi = 580 \times 288 \times 512$ . The grid extends from  $r \in [1.1525, 1000]r_g$ ,  $\theta \in [0, \pi]$  and  $\varphi \in [0, 2\pi]$ . In order to speed up our simulations, we redefine the  $\varphi$ -resolution by a factor of 4 near the polar axis. We checked the evolution of non-spinning BHs for an aligned disk (i.e., the disk midplane coincides with  $\theta = \pi/2$ ) and a highly misaligned disk, where the disk midplane coincides with the polar axis (see A 6.2) and found that the disk evolution is not affected when crossing the polar axis. We adopt outflowing radial boundary conditions (BCs), transmissive polar BCs and periodic BCs in the  $\varphi$ -direction (Liska et al. 2018, 2022).

We simulated a suite of accretion systems with the disk midplane misaligned at a variety of tilt angles,  $\mathcal{T}_{\text{disk}} = (0, \pi/2)$ , set by the BH and disk midplanes. Table 1 shows a summary of our model set, in which we follow the following naming convention:  $\text{T}\mathbf{x}$ |suffix $_i$ , where "x" denotes the initial disk tilt angle, and the suffix gives additional information about the model. We initialize the disk as an equilibrium hydrodynamic torus (Fishbone & Moncrief 1976) around a BH with a fiducial spin value of  $a = 0.9375$ . We set up a standard MAD magnetic field configuration (e.g., Chatterjee & Narayan 2022). For our gas thermodynamics, we assume an ideal gas equation of state with an adiabatic index of 13/9. The magnetic field strength is normalized by setting the ratio of maxima between the gas and magnetic pressures to 100. For tackling the evacuated region in the jet funnel, we adopt the density floor injection scheme of Ressler et al. (2017) when the magnetization exceeds 20. Figure 1 shows the initial disk setup, and its late-stage evolved state.

## 3. RESULTS

Our first set of fiducial model set comprises of 7 GRMHD simulations of varying initial disk inclinations evolved to  $\gtrsim 0.8 - 1 \times 10^5 r_g/c$ . At these late times, the radial profiles of different disk properties, such as the disk tilt angle  $\mathcal{T}$ , become roughly independent of time, and so the bulk of the disk achieves quasi-steady state behavior. Table 1 shows a summary of the simulation properties and some relevant time-averaged quantities for our models.

### 3.1. Moderately misaligned flows and magneto-spin alignment of the disk

First, we discuss the moderately misaligned disk simulations (models T15 to T60). The top panel of Fig. 2 shows the mass accretion rate  $\dot{M} = -\iint \rho u^r \sqrt{-g} d\theta d\varphi$  of the incoming flow, the dimensionless magnetic flux  $\phi_{\text{BH}} = 0.5\sqrt{4\pi/\dot{M}} \iint_{r=r_h} |B^r| \sqrt{-g} d\theta d\varphi$ , evaluated at the event horizon  $r_h = r_g(1 + \sqrt{1 - a^2})$ , and the outflow power efficiency  $\eta_{\text{out}} = P_{\text{out}}/\dot{M} = 1 - \dot{E}/\dot{M}$ , for two of the misaligned models, T45 and T60. Here we use the energy flux  $\dot{E} = \iint T_t^r \sqrt{-g} d\theta d\varphi$ , where  $T_t^\mu$  is the stress-energy tensor. Here  $g$  is the metric determinant. We calculate both  $\dot{M}$  and  $\dot{E}$  at  $r = 5r_g$  so as to avoid contamination due to density floors.

In Fig. 2, despite the difference in the initial disk inclination ( $45^\circ$  versus  $60^\circ$ ), the  $\dot{M}$ ,  $\eta_{\text{out}}$  and  $\phi_{\text{BH}}$  of the two models evolve very similarly over time. The outflows from both models exceed efficiencies of 100% and the accretion flow at small radii reaches magnetic flux saturation, indicated by the time-averaged magnetic flux

Tilt Model	Magnetic field	BH spin	$\mathcal{T}_{\text{disk}}^{\circ}$ (initial)	Resolution $N_r \times N_{\theta} \times N_{\varphi}$	$t_{\text{sim}}$ [ $10^4 r_g/c$ ]	$\langle \phi_{\text{BH}} \rangle$ ( $r = r_h$ )	$\langle \eta_{\text{out}} \%$	$\langle \mathcal{T}_{\text{disk}}^{\circ} \rangle$ ( $10 r_g$ )	$\langle \mathcal{T}_{\text{disk}}^{\circ} \rangle$ ( $150 r_g$ )	$\langle \mathcal{T}_{\text{jet}}^{\circ} \rangle$ ( $10 r_g$ )
Fiducial models: Tilted MADs										
T0	MAD	0.9375	$0^{\circ}$	$580 \times 288 \times 512$	8.27	61.2	190.5	2.7	1.8	$5.61 \pm 2.56$
T15	MAD	0.9375	$15^{\circ}$	$580 \times 288 \times 512$	13.4	60.4	191.4	2.62	8.07	$5.72 \pm 3.84$
T30	MAD	0.9375	$30^{\circ}$	$580 \times 288 \times 512$	11.4	59.9	187.8	2.83	14.9	$7.06 \pm 4.39$
T45	MAD	0.9375	$45^{\circ}$	$580 \times 288 \times 512$	12.9	62.2	198.2	2.61	23.2	$6.46 \pm 2.95$
T60	MAD	0.9375	$60^{\circ}$	$580 \times 288 \times 512$	12.4	60.8	190.5	2.5	27.4	$5.26 \pm 2.11$
T75	MAD	0.9375	$75^{\circ}$	$580 \times 288 \times 512$	9.7	18	3.139	78.2	74.8	$76.7 \pm 6.79$
T90	MAD	0.9375	$90^{\circ}$	$580 \times 288 \times 512$	10.1	19.1	4.257	80.6	71.5	$75.8 \pm 8.81$
T90H	MAD	0.9375	$90^{\circ}$	$696 \times 576 \times 576$	7.33	18	4.66	84.2	77.1	$80.2 \pm 5.55$
T90L <sup>†</sup>	MAD	0.9375	$90^{\circ}$	$1160 \times 192 \times 384$	10.2	16.8	18.38	58.8	81	$21.7 \pm 15.9$
Tilted MAD models with alternate black hole spin										
T30A5	MAD	0.5	$30^{\circ}$	$580 \times 288 \times 512$	5	57.4	26.56	11.4	25.1	$12.1 \pm 3.24$
T30A5M	MAD	-0.5	$30^{\circ}$	$580 \times 288 \times 512$	5	33.1	6.136	38.5	31.3	$31.5 \pm 3.89$
T30A93M	MAD	-0.9375	$30^{\circ}$	$580 \times 288 \times 512$	5	19.7	8.084	44.1	36.2	$32.9 \pm 6.23$
Tilted Near-MAD models based on <a href="#">Liska et al. (2018)</a> and <a href="#">Chatterjee et al. (2020)</a>										
T0-S	Strong	0.9375	$0^{\circ}$	$448 \times 144 \times 240$	13.2	52.8	140.4	3.57	1.84	$5.77 \pm 2.28$
T30-S	Strong	0.9375	$30^{\circ}$	$448 \times 144 \times 240$	11.9	46.3	102	20.7	21.8	$18.2 \pm 2.99$
T60-S	Strong	0.9375	$60^{\circ}$	$448 \times 144 \times 240$	14.8	33.3	47.5	42.7	41.8	$33.3 \pm 3.23$
T30A5-S	Strong	0.5	$30^{\circ}$	$448 \times 144 \times 240$	11	49.9	21.76	24	25.2	$23.9 \pm 3.36$
T30A93M-S	Strong	-0.9375	$30^{\circ}$	$448 \times 144 \times 240$	5	12.7	7.309	22.6	33.6	$23.9 \pm 1.42$
Tilted BH models for alternate initial conditions (See Sec. 6.1)										
TOBH	MAD	0.9375	$0^{\circ}$	$580 \times 192 \times 384$	5	54.3	143.3	3.02	6.37	$7.05 \pm 3.92$
T60BH	MAD	0.9375	–	$580 \times 192 \times 384$	5	25	30.1	42.6	66.8	$46.8 \pm 20.9$
T90BH	MAD	0.9375	–	$580 \times 192 \times 384$	5	23.2	15.21	28	27.5	$35.5 \pm 12$
T90BHb	MAD	0.9375	–	$580 \times 192 \times 384$	5	9.25	0.8024	26.4	26.9	$34.5 \pm 19$

**Table 1.** Summary table for all numerical simulations used in this work. We mention the model names, the magnetic field configuration for the initial disk (either a MAD or a strongly magnetized disk), initial disk tilt angle ( $\mathcal{T}_{\text{disk}}$ ), simulation grid resolution and simulation end time  $t_{\text{sim}}$ . We include time-averaged simulation quantities: mass accretion rate  $\dot{M}$ , dimensionless magnetic flux  $\phi_{\text{BH}}$ , outflow efficiency  $\eta_{\text{out}}$ , and the final disk tilt angles  $\mathcal{T}_{\text{disk}}$  at  $10 r_g$  and  $150 r_g$  (indicating the inner and outer disks). We average the simulation quantities over the final  $10^4 r_g/c$  for each simulation.

<sup>†</sup> Note that T90L has an outer boundary of  $10^6 r_g$ .

$\langle \phi_{\text{BH}} \rangle \gtrsim 50$  and the clear presence of dips in the magnetic flux and accretion rate due to magnetic flux eruptions in the time plots. Indeed, models T15–60 all develop the MAD state ( $\phi_{\text{BH}} \gtrsim 50$ ) and exhibit highly efficient outflows, similar to the non-tilted T0 MAD model (see Table 1), and typical of geometrically thick MAD flows around rapidly-spinning prograde BHs (both  $\phi_{\text{BH}}$  and  $\eta_{\text{out}}$  depends on the BH spin and the disk scale-

height; e.g. [Tchekhovskoy et al. 2012](#); [Narayan et al. 2022](#); [Lowell et al. 2023](#)).

For all of the moderately tilted disk models, as the accretion flow develops the MAD state, the strongly magnetized jet is able to generate enough electromagnetic torque to force the inner disk flow to align with the black hole spin axis. The “magneto-spin alignment” of the disk results in near-zero values of the disk tilt angle

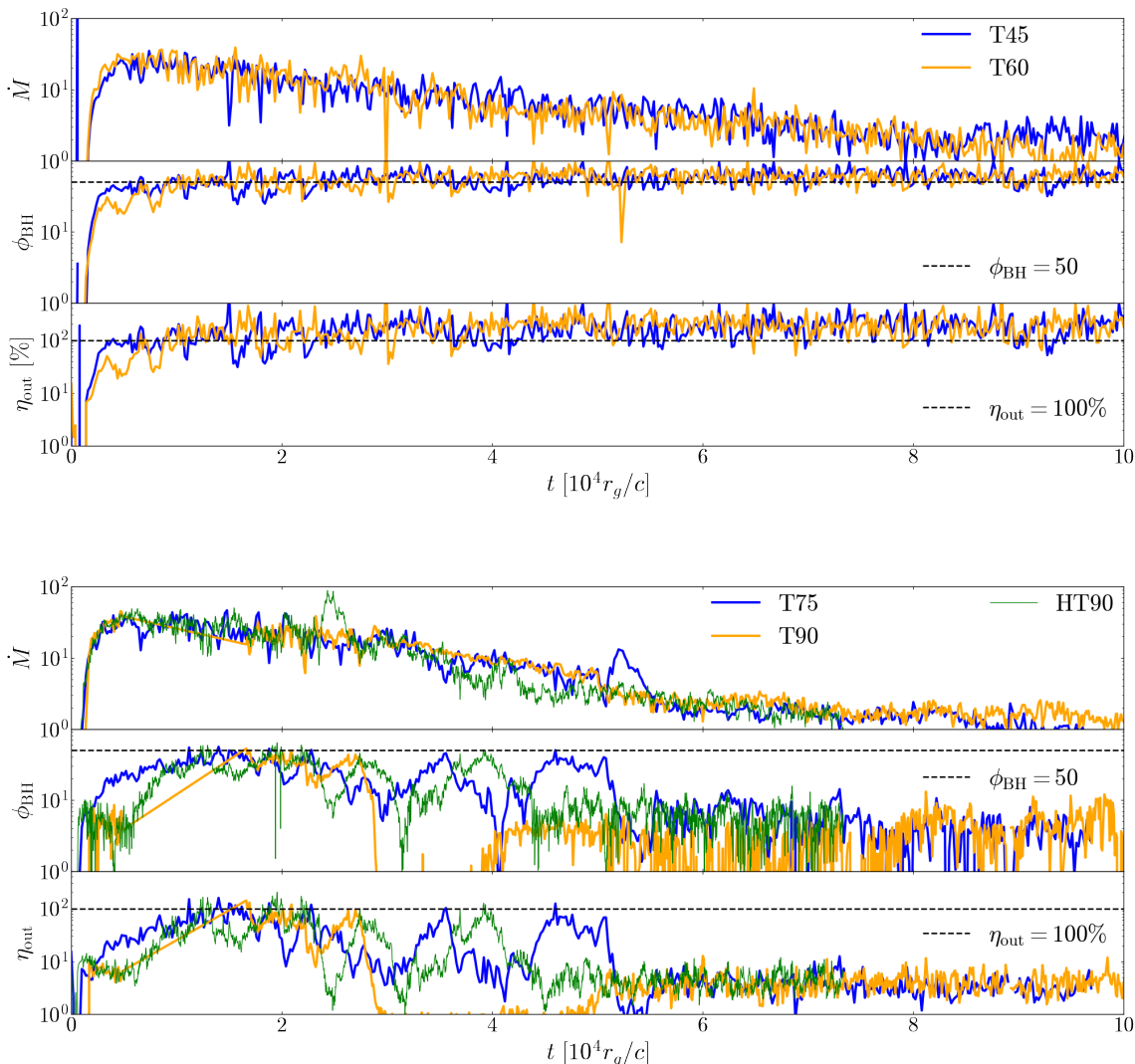


**Figure 2.** Disks with initial tilt angles smaller than  $60^\circ$  develop the MAD state, while highly tilted disks undergo rapid transitions in magnetic flux and outflow power. We show the temporal evolution of the accretion rate  $\dot{M}$  (in code units), the dimensionless magnetic flux  $\phi_{\text{BH}}$  and the outflow efficiency  $\eta_{\text{out}} = P_{\text{out}}/\dot{M}$  for moderately-misaligned disks T45 and T60 (top) and highly-misaligned disks T75 and T90 (bottom). We also include T90H, a higher resolution version of T90.

close to the BH (shown at a radius of  $10 r_g$  in Fig. 3, top panel) over time. On the other hand, the bottom panel of Fig. 3 shows that at larger distances from the BH (specifically  $r = 150 r_g$  in the plot), the outer disk undergoes relatively smaller levels of alignment. Figure 4 shows the radial profile of the disk tilt angle, averaged over the final  $20000 r_g/c$ . The moderately misaligned disks exhibit near-perfect alignment with the BH spin axis at least out to  $10 r_g$ , beyond which the flow remains misaligned. It is possible that the alignment radius increases out to large radii over several viscous timescales, depending on whether the flow angular velocity remains sub-Keplerian (McKinney et al. 2013). We also note

that the jet torque roughly realigns the inner disk to its final orientation within the first  $10^4 r_g/c$  of its evolution, much faster than the BP alignment timescales.

### 3.2. Extremely misaligned disks and the intermittent ejection of jets

The extremely tilted disk models T75 and T90, with initial disk misalignment angles of  $75^\circ$  and  $90^\circ$  respectively, evolve entirely differently from the moderate spin cases. Focusing on the late time-averaged properties first, these two models do not end up in a quasi-steady MAD state, but instead exhibit a weakly magnetized accretion flow. The models show a dimensionless magnetic flux  $\langle \phi_{\text{BH}} \rangle \lesssim 6$  (Fig. 2 and Table 1) along with weakly

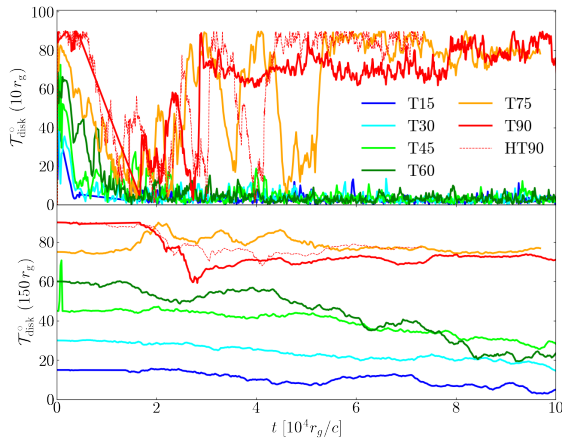


**Figure 3.** We show the disk tilt angle for our fiducial tilted MAD simulations at  $10 r_g$  (top) and  $150 r_g$  (bottom). Disks that develop the MAD state (Fig. 2) exhibit strong alignment with the BH spin while highly tilted disks show periods of alignment for the inner disk when the magnetic flux is large enough to produce a jet.

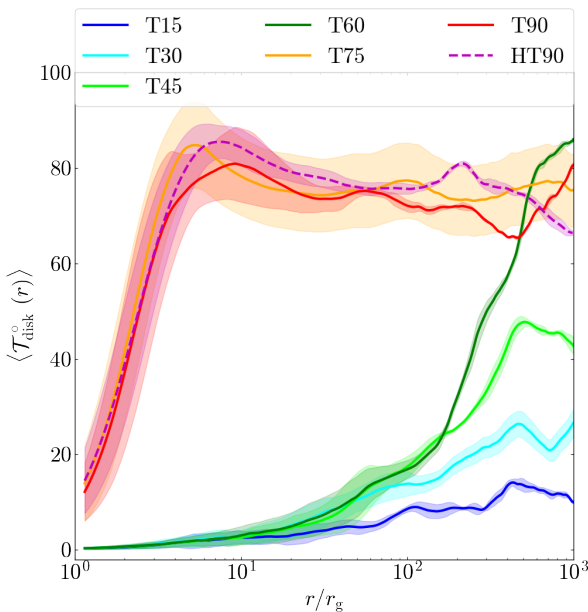


**Figure 4.** Radial profiles of the disk tilt angle for our fiducial models, time-averaged over the final  $20,000 r_g/c$ . Moderately tilted disks show strong alignment at least to radius  $r \gtrsim 10 r_g$  while highly tilted disks exhibit radial tilt oscillations as expected for weakly magnetized tilted disks (e.g., Liska et al. 2018).

powered jets with efficiencies of a few per cent. In these models, magneto-spin alignment of the disk does not seem to occur: the tilt angle of the inner disk stabilizes to  $\sim 80^\circ$  (from Fig. 3). Indeed, the radial profile of the disk tilt angle (Fig. 4) exhibits radial tilt oscillations reminiscent of relatively weakly magnetized misaligned accretion flows (as seen in, e.g., Fragile et al. 2007; Liska et al. 2018; White et al. 2019; Chatterjee et al. 2020); the strong disk alignment only occurs within a few gravitational radii from the BH.

Despite starting with physical conditions conducive to forming a MAD state, why do our extremely misaligned disks somehow appear similar to their weakly magnetized cousins? The answer hides in their time evolution. Figure 2 shows that both T75 and T90 reaches  $\phi_{\text{BH}} \approx 50$  along with relatively high outflow efficiencies (indicative of powerful jets) around  $2 \times 10^4 r_g/c$ . Just beyond this point, at  $t \sim 2 - 6 \times 10^4 r_g/c$ , both  $\phi_{\text{BH}}$  and  $\eta_{\text{out}}$  show rapid variability and eventually settle to low values that are representative of weakly magnetized disks. The outflow power profile follows the magnetic flux as the jet is powered via the Blandford & Znajek (1977) mechanism:  $\eta_{\text{jet}} \propto a^2 \phi_{\text{BH}}^2$ . The temporal profile of the inner and outer disk tilt angles in Fig. 3 replicates the highly variable behavior of  $\eta_{\text{out}}$  since whenever the jet power increases, the torque on the disk due to the jet becomes large enough to activate magneto-spin alignment, decreasing the disk tilt angle.

To make sure that our results are independent of grid resolution, we ran a higher resolution version of T90, called T90H with double the number of grid cells in  $\theta$ -direction to ensure that the accretion flow is very well-resolved even near the grid polar axis region. We find that the fiducial and high resolution models evolve similarly in time and show converged disk tilt angle profiles (Figs. 2, 3 and 4). However, we note that transient jetted phase of T90H shows more high-power ejection events as is evident from the presence of peaks in  $\eta_{\text{out}}$  at  $t \sim 3 - 5 \times 10^4 r_g/c$  in Fig. 2. Additionally, we have performed grid tests for Schwarzschild BHs with disks aligned with the  $\theta = 0$  and  $\theta = \pi/2$  planes and found that our disks evolve similarly, providing confidence in our base grid resolution (see Appendix 6.2).

What causes the variability in the magnetic flux and further, why does it settle down to such low values at late times? To answer this question, in Fig. 5, we construct space-time evolution plots of the outflow power efficiency  $\eta_{\text{out}}$ , the disk tilt angle  $\mathcal{T}_{\text{disk}}$ , and the disk poloidal magnetic flux, defined as  $\Phi(r) = \max_r \Phi_p(r)$  with  $\Phi_p(r) = \max_{\tilde{\theta}} \iint_0^{\tilde{\theta}} B^r(r, \tilde{\theta}, \tilde{\varphi}) \sqrt{-g} d\tilde{\theta} d\tilde{\varphi}$  (e.g., Liska et al. 2019). Here, the “tilde” denotes rotated spherical polar coordinates such that the coordinate frame is

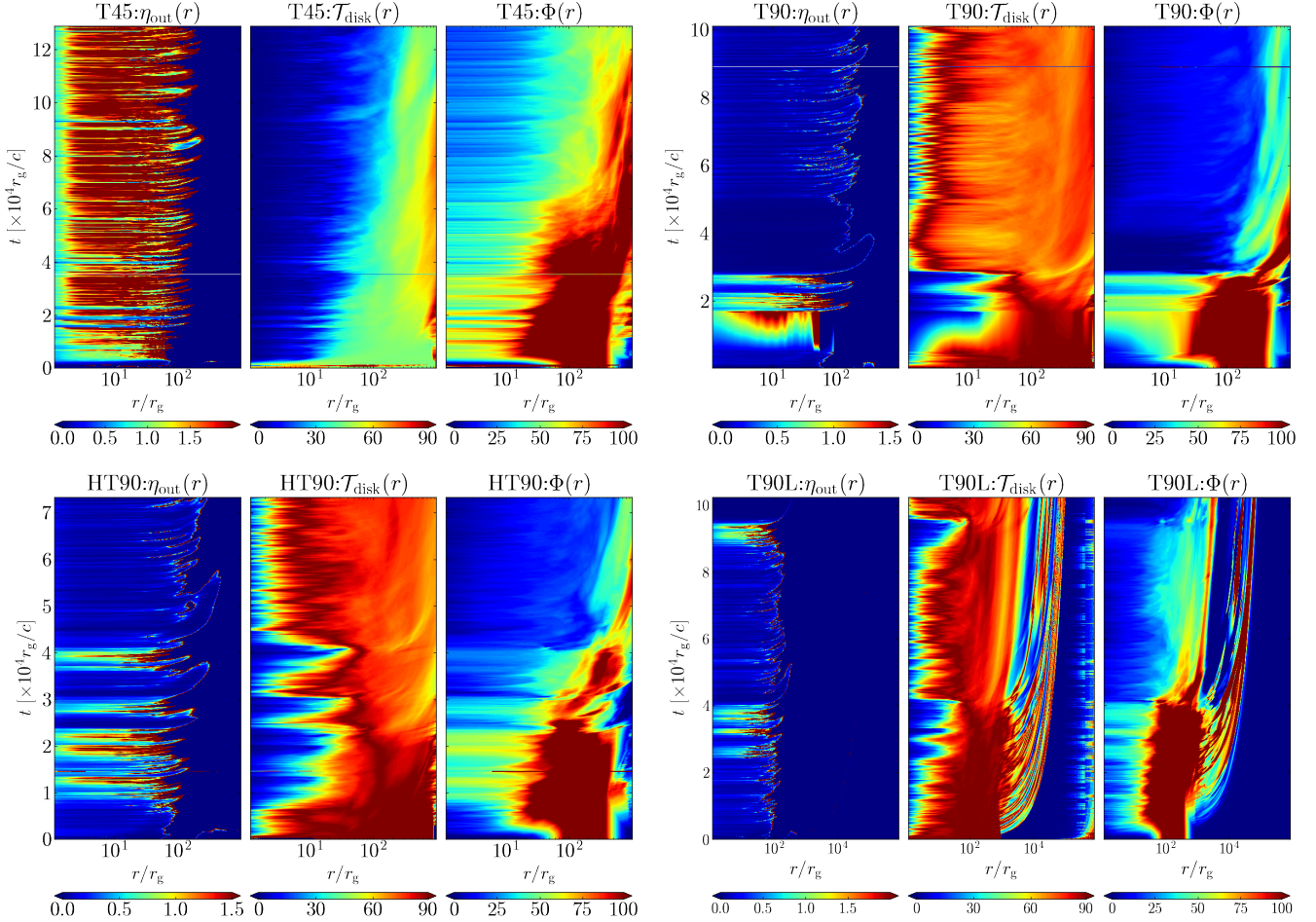


**Figure 5.** We show the time and radial evolution of the outflow power  $\eta_{\text{out}}$ , and its relation to the disk tilt angle  $\mathcal{T}_{\text{disk}}$  and the enclosed magnetic flux  $\Phi$  in the disk for models T45, T90, T90H and T90L. We see that intermittent jets, indicated by periods of large outflow power, force the disk to align with the BH’s spin axis. However, due to strong collisions between the disk and the jets, magnetic flux gets ejected out to large radii, consequently resulting in weakened outflows with  $\eta_{\text{out}} \ll 10\%$ .

aligned with the disk angular momentum vector at every radius  $r$ .

The space-time plots show that jet production in these models is intermittent and the disk orientation undergoes rapid changes depending on the strength of the magnetic flux near the BH horizon. Whenever there is enough magnetic flux on the BH horizon to launch a jet, these jets not only force the disk into alignment with the BH spin (indicated by the sharp reduction in  $\mathcal{T}_{\text{disk}}$  when  $\eta_{\text{out}}$  is large) but also inadvertently collide with the disk bulk. These jet-disk collisions push gas and magnetic flux outwards, which depletes  $\phi_{\text{BH}}$  and reduces jet power. As the jet power reduces in strength, the angular momentum vector of the accreting gas in the inner disk switches back to that of the large scale disk. Over time, magnetic flux re-accumulates near the BH, relaunching the jets. This oscillatory behavior in the inner disk tilt angle continues until enough magnetic flux has escaped the simulation domain and

the disk reaches a quasi-steady state warped structure reminiscent of weakly magnetized misaligned accretion flows seen in Chatterjee et al. (2020), typically dubbed as “SANE” accretion flows in GRMHD literature (e.g., Narayan et al. 2012; Porth et al. 2019).

In both T75 and T90 models, any outflows, when generated, push the bulk of the available gas and magnetic flux out to large radii and eventually out of the simulation domain that extends out to  $r = 10^3 r_g$ . This behavior is confirmed by the higher resolution simulation T90H, increasing confidence in our results. Such a result is a feature of both the (relatively) small outer radial boundary of  $r = 10^3 r_g$  and our use of outflow radial boundary conditions that do not resupply the simulation domain with any additional gas or magnetic flux over time as opposed to Bondi-Hoyle-Lyttleton (Hoyle & Lyttleton 1939; Bondi & Hoyle 1944; Edgar 2004) type models (e.g., quasi-spherical rotating inflows or wind-fed inflows; Ressler et al. 2020; Lalakos et al. 2022) where a

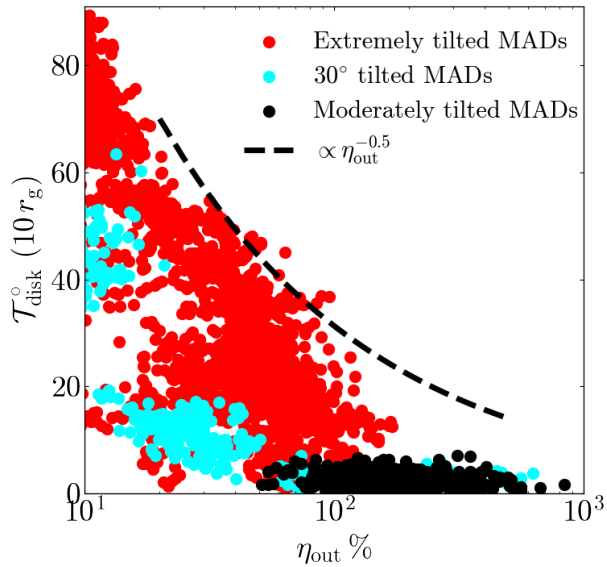


**Figure 6.** Magneto-spin alignment in misaligned disks: the higher the outflow power, the stronger the disk/jet alignment. We show the disk tilt angle as a function of the outflow power  $\eta_{\text{out}}$  during different times of evolution for our fiducial models (“Moderate” and “Extreme” cases) as well as  $30^\circ$ -tilted MAD models with alternate BH spins. The magneto-spin alignment mechanism provides an upper limit on the maximum disk tilt angle for a specific jet power.

common choice is to fix the magnetic field at the outer radial boundary of the simulation domain.

To eliminate the effect of a finite outer radial boundary, we move it to  $10^6 r_g$  and to keep the same radial grid resolution as the T90 model, we double the number of cells in the  $r$ -direction. The resulting simulation, T90L, exhibits the same expulsion of the magnetic flux from the inner disk due to jet-disk collisions as seen for models T90 and T90H in Fig. 5 at  $t \sim 4 \times 10^4 r_g/c$ . Because of the larger domain size in model T90L, the expelled flux remains within the simulation domain and advects inwards along with the gas on a viscous timescale and finally accumulates near the BH. This results in a restarted jet at  $t \sim 9 \times 10^4 r_g/c$ . After another bout of powerful jet production, the magnetic is re-expelled and the whole cycle begins anew. This is the first demonstration of self-quenching of the MAD state and the production of restarted jets in thick accretion flows.

### 3.3. Jet power efficiency and disk alignment

Fig. 5 also shows the evolution of model T45 where the disk misalignment angle is small enough for the jets to avoid significant collisions with the disk, and therefore, magnetic flux sufficiently large enough to power MAD

jets is always present near the BH. For such small misaligned disks, the magneto-spin alignment radius ( $r_{\text{msa}}$ ) seems to grow with time until a distance where the jet torque equals the large scale disk torque (McKinney et al. 2013; Polko & McKinney 2017) that depends on both the BH spin  $a$ , the poloidal magnetic flux both supplied by the disk and accumulated at the BH, the accretion rate as well as the angular velocity of the accreting gas,

$$r_{\text{msa}} \propto \frac{a\Phi^2}{\dot{M}v_\varphi}. \quad (1)$$

Thus the alignment radius strongly depends on the distance to which the disk is magnetically dominated (called the MAD saturation radius  $r_{\text{MAD}}$ ; e.g., Narayan et al. 2003; McKinney et al. 2012; Begelman et al. 2022; Chatterjee & Narayan 2022) as, for a given radius  $r$ , such a disk would not only have the maximum possible disk magnetic flux but also the minimum possible accretion rate and gas angular velocity since stronger magnetic fields suppress  $\dot{M}$  (e.g., Lalakos et al. 2022) and provide support to the disk against gravity, resulting in a highly sub-Keplerian disk angular velocity (e.g., Chatterjee & Narayan 2022). It is presently unknown what dictates the MAD saturation radius and how far out can it reach, with current simulations suggesting  $r_{\text{MAD}} \gtrsim 40 - 100 r_g$ . The moderately-misaligned MAD simulations in this work certainly show significant disk alignment out to  $100 r_g$ , where the disk is at least partially magnetically saturated.

From the above discussion, it is clear that the magneto-spin alignment radius  $r_{\text{msa}}$  is a non trivial quantity to compare between simulations. Instead of  $r_{\text{msa}}$ , in Fig. 6, we check the dependence of  $\mathcal{T}_{\text{disk}}$ , evaluated at  $r = 10 r_g$ , on  $\eta_{\text{out}}$  since the alignment mechanism directly depends on the torque exerted by the jet on the disk. For the moderately-misaligned disk models, the MAD state develops quickly and the alignment of the inner disk ( $r \approx 10 r_g$ ) occurs within the first  $10^4 r_g/c$  of the simulation (as seen from Fig. 3). This is why these particular models (black circles) cluster near  $\mathcal{T}_{\text{disk}} \approx 0^\circ$  and  $\eta_{\text{out}} \gtrsim 100\%$ . On the other hand, the extremely misaligned models (red circles) exhibit an incredibly large variation of disk and jet morphologies, spanning almost all possible values of disk tilt angles and jet efficiencies, bounded from above by the relation  $\mathcal{T}_{\text{disk,max}} \propto 1/\sqrt{\eta_{\text{out}}}$ .

We include three additional  $30^\circ$  tilted MAD disk simulations varying the BH spin direction and magnitude:  $a = \pm 1/2$  and  $-0.9375$ , indicated by cyan circles in Fig. 6 (including the previously mentioned T30 simulation). We provide more details about the simulations in Table 1. These simulations exhibit partial alignment of

the inner disk even in the MAD state. Figure 6 shows that the jet efficiencies from these BH disks are relatively small ( $\eta_{\text{out}} < 60\%$ ) compared to the  $a = +0.9375$ ,  $30^\circ$  tilted disk model. Thus the resultant jet torque is not strong enough to align the disk with the BH symmetry plane and the disk tilt angle falls well below the  $1/\sqrt{\eta_{\text{out}}}$  upper bound.

Given the above results, we suggest that the jet efficiency upper bound is a universal relation due to the magneto-spin alignment mechanism, independent of BH spin and initial disk misalignment angle. Even under the condition of abundant supply of magnetic flux to the BH, the accretion flow within the inner  $10 r_g$  of the BH (and therefore, also the jet base) cannot be misaligned with the BH spin axis by an angle larger than  $\mathcal{T}_{\text{disk}/\text{jet},\text{max}} \approx 70^\circ \sqrt{20\%/\eta_{\text{out}}}$ . We expect such a relation to also hold for BHs accreting at larger accretion rates as  $\eta_{\text{out}}$  typically decreases for smaller disk scale heights. At sufficiently large accretion rates ( $\dot{M} \gtrsim 0.1\%$  of the Eddington accretion rate), the disk scale height becomes smaller than the effective disk viscosity and the alignment process changes from magneto-spin to the Bardeen-Petterson alignment process where viscous dissipation damps out radial tilt oscillations in the disk (Bardeen & Petterson 1975; Polko & McKinney 2017; Liska et al. 2019).

### 3.4. Jet power with misaligned disks

One of the most important attributes of the MAD state is the production of powerful jets with efficiencies  $\eta_{\text{out}} > 100\%$  when the BH spin  $a \gtrsim 0.8$  (Tchekhovskoy et al. 2011, 2012; Narayan et al. 2022). The moderately misaligned disk models in our fiducial model set (T15-T60) exhibited magneto-alignment of the inner disk and reached the MAD state with outflow efficiencies exceeding 100% (Table 1). The highly misaligned models, on the other hand, showed weakly powered jets ( $\eta_{\text{out}} \lesssim 5\%$ ), due to the lack of sustained jet production. Thus, our results suggest that, given enough magnetic flux supply, for initial disk misalignment angles  $\lesssim 60^\circ$ , magneto-alignment of the inner disk due to the emergence of the MAD state would result in jet efficiencies equivalent to the MAD limit for the corresponding aligned disk model.

However, for misaligned disks that are initialized with strong poloidal magnetic fields but not enough magnetic flux to reach the MAD state (hereafter called “strong-field” models), the disk bulk exhibits radial tilt oscillations. Only the inner disk undergoes partial alignment with the BH spin and accretion occurs via plunging streams. To show what happens to  $\phi_{\text{BH}}$  and  $\eta_{\text{out}}$  for strong-field misaligned disks, we include 3 misaligned

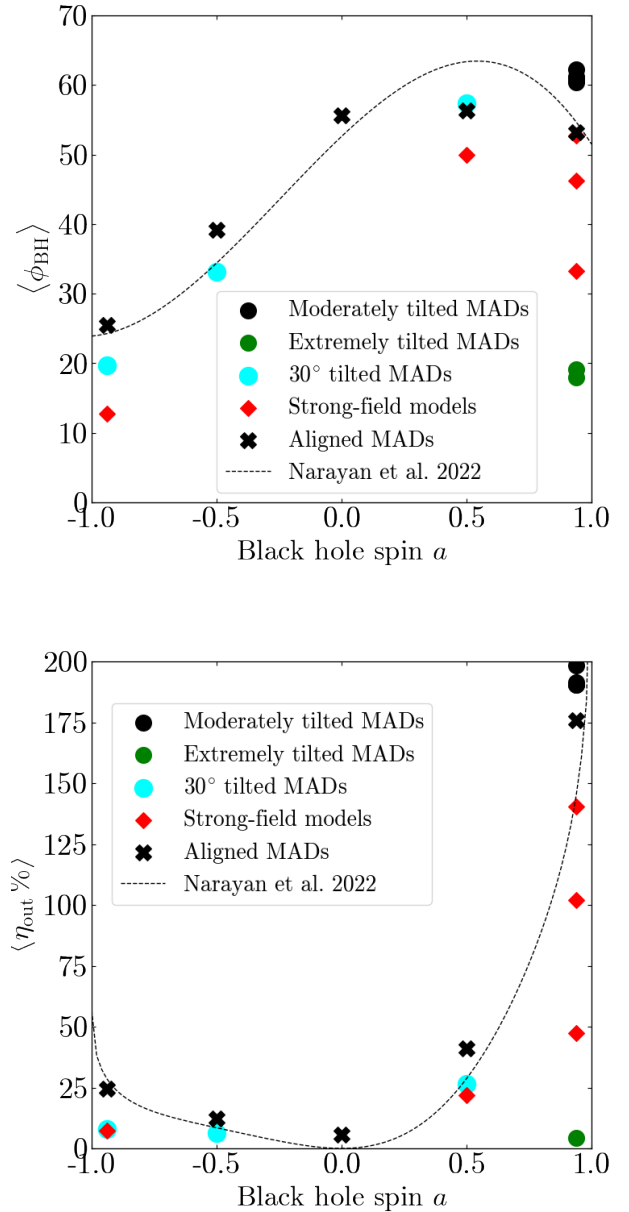


**Figure 7.** Normalized magnetic flux at the horizon (top) and Outflow efficiency plot (bottom) for all models, time-averaged over the final  $10^4 r_g/c$  of each simulation.

disk models with BH spin  $a = 0.9375$  from Liska et al. (2018) and Chatterjee et al. (2020) - for initial disk misalignment angles of  $0^\circ$  (T0-S),  $30^\circ$  (T30-S) and  $60^\circ$  (T60-S)<sup>1</sup>. In addition, we include two previously unpublished simulations from the strong-field model set

<sup>1</sup> These models are referred to as T0, T30 and T60 respectively in Chatterjee et al. (2020).

where the initial disk tilt is  $30^\circ$  but the BH spin is  $a = 0.5$  (T30A5-S) and  $a = -0.9375$  (T30A93M-S). Table 1 shows a summary of the simulation parameters. Further details about the simulations are given in Liska et al. (2018) and Chatterjee et al. (2020). For comparison, we also included a series of aligned MAD simulations with BH spins  $a = 0, \pm 0.5, \pm 0.94$  from the H-AMR EHT simulation library (Event Horizon Telescope Collaboration et al. 2022) as well as the fits for  $\phi_{\text{BH}}$  and  $\eta_{\text{out}}$  in the aligned MADs from Narayan et al. (2022).

Figure 7 shows the normalized magnetic flux at the event horizon,  $\phi_{\text{BH}}$ , and the outflow power efficiency,  $\eta_{\text{out}}$ , for both the MAD and the strong-field models. First, as expected, the moderately-misaligned MAD models show similar magnetic flux and jet power values as the aligned models while the extremely-misaligned models are flux-depleted and therefore, host very weak jets. Second, for the  $a = 0.9375$  strong field models, the magnetic flux (and thus, the jet power as well) decreases significantly with increasing initial disk angle. In these models, the warping of the accretion flow prevents efficient accumulation of magnetic flux near the BH (i.e., the warped disk is unable to “hold on” to the magnetic flux as effectively as in aligned disks).

Next, for low-spin BHs ( $a = 0, \pm 1/2$  in our model set), we see little-to-no difference between the aligned and misaligned disk  $\phi_{\text{BH}}$  and  $\eta_{\text{out}}$  values as the Lense-Thirring torque is either too small or absent. Additionally the resultant jets are too weak to force the disk into alignment (which also supports the  $\mathcal{T}_{\text{disk,max}} \propto 1/\sqrt{\eta_{\text{out}}}$  relation introduced in the previous subsection). Finally, for rapidly spinning retrograde BHs, we again see that disk warping lowers the magnetic flux value compared to aligned MADs, producing weak jets that are unable to magneto-align the disk as  $\eta_{\text{out}} \approx 10\%$ . Overall, we find that introducing misaligned accretion lowers the magnetic flux and the jet power in high spin (prograde or retrograde) BHs as Lense-Thirring torques are large enough to warp the disk with the exception of high spin prograde MADs when the jet can become strong enough to magneto-spin-align the disk.

## 4. ASTROPHYSICAL IMPLICATIONS

### 4.1. Shock-heating during jet-disk collisions

Our simulations reveal two exciting regimes of misaligned accretion, (1) one where the torque due to the jet dominates over the accretion flow, forcing the inner disk into alignment with the BH spin axis at least within a few tens of gravitational radii from the BH, and (2) the other where jet ejection is intermittent in nature and leads to a rapid re-orientation of the accretion flow. While the first regime, seen for MAD disks with

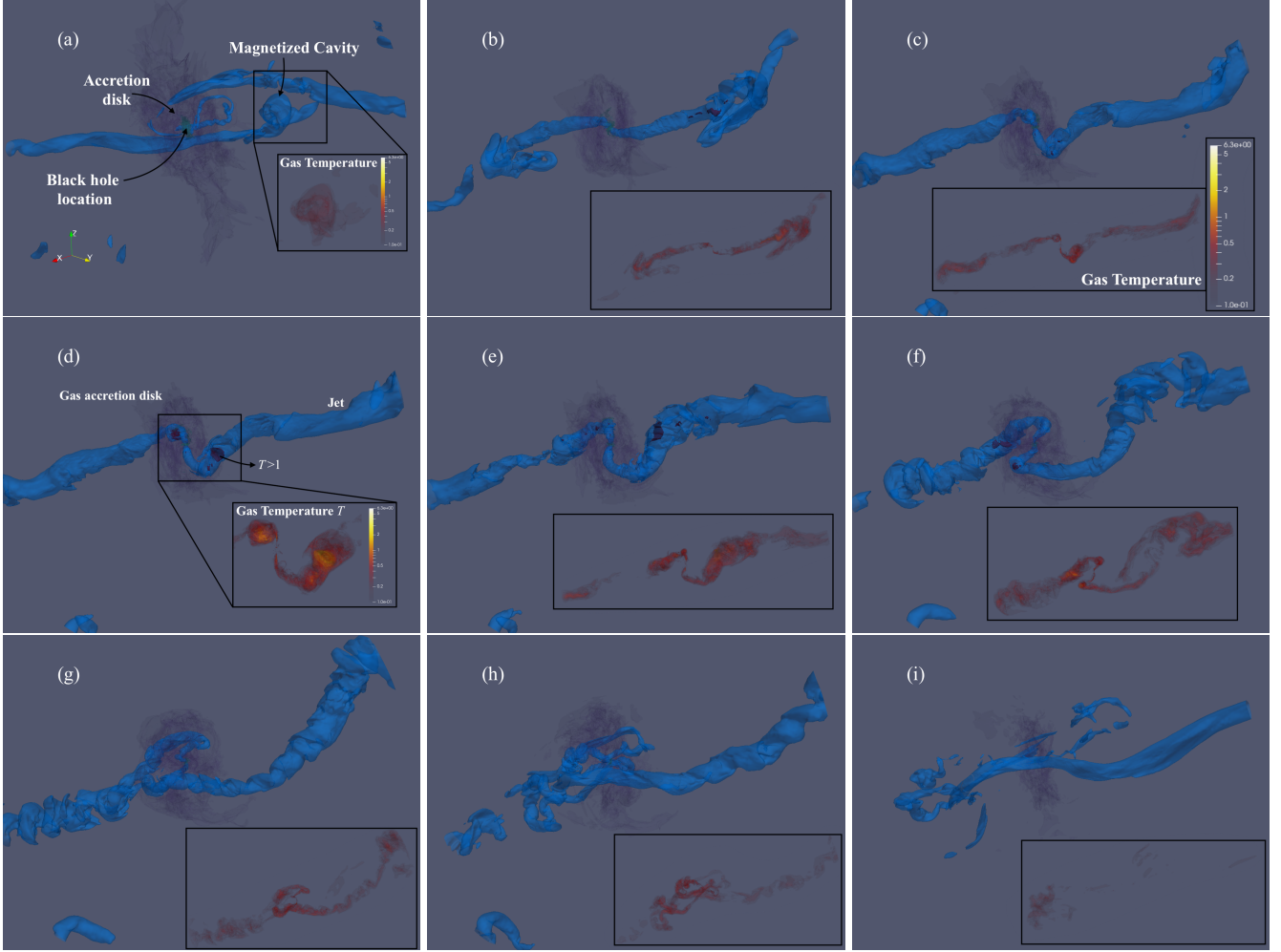
$\mathcal{T}_{\text{disk}} \lesssim 60^\circ$ , resembles aligned MAD accretion, the extreme misaligned disks with  $\mathcal{T}_{\text{disk}} \gtrsim 70^\circ$  exhibit a variety of disk/jet morphologies, especially during outbursts.

Figure 8 shows the evolution of one such outburst phase seen in the high resolution model T90H, with the initial disk tilt,  $\mathcal{T}_{\text{disk}} = 90^\circ$ . In Fig. 8(a), we start with a snapshot in time when the jet is inactive, but the environment is filled with filamentary magnetized remnants (in blue) from a previous outburst. These remnants, at times, are also filled with near-relativistically hot plasma (with  $\Theta \equiv k_B T_{\text{gas}}/mc^2 \gtrsim 0.1$ ) and buoyantly rise outwards, resembling hot cavities often seen in AGN (e.g., Ubertosi et al. 2021). Once enough magnetic flux accumulates at the BH event horizon, the jet relaunches. This can be seen in Fig. 8(b) where the bipolar structure of the restarted jet is clearly seen pushing out the disk and pre-existing jet remnants. There are also hints of short-lived jet precession from the clockwise movement of the jet base during this early jet ejection phase.

Over time, as the BH horizon magnetic flux increases, the jet grows in strength and tends to align with the vertical BH spin axis, thus forcing the disk into alignment, launching the magneto-spin alignment process. Figure 8(c,d) shows the jets, as they punch through the disk leaving the large-scale jet in a completely different orientation compared to the small-scale jet. The jet-disk collisions result in regions of super-heated shocked gas (of relativistic gas temperatures  $\Theta > 1$ ), potentially being zones of hard X-ray and possibly even  $\gamma$ -ray emission.

As we saw in Sec.3.2, in colliding with the accreting gas, the jet disrupts its own supply of gas and magnetic flux and triggers a series of severe kink instabilities that cause the jet to wobble vigorously (Fig. 8e,f) and eventually disrupt (Fig. 8g,h). Thus the system returns to the state it started with: quasi-spherical weakly-magnetized accreting gas with disordered magnetized filaments and plumes of hot gas, remnants of a self-destructed jet (Fig. 8i).

Our larger scale simulation, T90L, showed that the gas and magnetic flux, ejected during the jet outburst ( $2.5 \times 10^4 r_g/c \lesssim t \lesssim 4 \times 10^4 r_g/c$ ), re-accumulates near the BH and restarts the outburst at  $t \sim 9 \times 10^4 r_g/c$ , or around 12 days later for Sagittarius A\*-like BHs and 50 years for M87-like BHs, with each outburst leading to pronounced X-ray flares. The self-consistent nature of the feedback mechanism could also exhibit quasi-periodicity in radio and X-ray eruptions, such as the recently discovered quasi-periodic eruption event of Swift J0230+28 (Evans et al. 2023; Guolo et al. 2023). For this particular source, the estimated BH mass between  $1.5 - 10$  million  $M_\odot$ , which gives us an approximate



**Figure 8.** 3D renderings of T90H during a jet ejection phase: the disk (indicated by gas density in green-purple) and the jet (indicated by the magnetization  $b^2/\rho c^2 = 1$  surface in blue). The insets show gas temperature in relativistic units ( $\Theta \equiv k_B T_{\text{gas}}/m_p c^2 \geq 1$  indicates relativistically-hot gas). The box size is the same as the simulation box (i.e., a sphere with a maximum radius of  $10^3 r_g$ ). The movie version is available at this [Youtube link](#)

periodicity of 4.3 to 28.6 days, consistent with the observed 22 day periodicity. We leave the necessary radiative transfer calculations for detailed comparisons to future work.

Other than these outbursts, separated by days to several years depending on the BH mass, steady jets, if present, are weakly powered ( $\eta_{\text{out}} \lesssim 5\%$ ) and may not provide any substantial radio emission, making such highly-misaligned systems good candidates for radio-quiet sub-Eddington AGN. The BZ jet power efficiency is given by  $\eta_{\text{BZ}} \propto a^2 \phi_{\text{BH}}^2$ . Thus, to explain the absence of a steady-powered, radio jet, either the BH spin magnitude must be small (as suggested by e.g., Tchekhovskoy et al. 2010) or the magnetic flux supply to the BH must be meager. While most BH spin measurements skew towards high spin values (Reynolds 2021), BHs in galaxies with significant merger activity may carry low spins. For the magnetic flux, the ISM supplies strong mag-

netic fields (plasma- $\beta \approx 1$ , e.g., Ferrière 2020), providing an environment favorable for the development of the MAD state. If the BH and disk angular momentum vectors are misaligned enough to allow for jet-disk collisions, both spin and magnetic flux constraints are unnecessary. Capturing radio-quiet AGN during outbursts would then be crucial to verifying whether such highly-misaligned BH systems are indeed viable in nature.

#### 4.2. Jet precession in highly sub-Eddington black holes

In this section, we discuss the Lense-Thirring (LT) precession of jets in the context of BHs accreting at highly sub-Eddington accretion rates,  $\dot{M} \ll 10^{-3} \dot{M}_{\text{Edd}}$ , when the accretion flow is still in the geometrically-thick advection-dominated regime, e.g., the quiescent and hard states in XRBs and low-luminosity AGN, before the inflow transitions to a truncated disk state (e.g., Fender et al. 2004; Liska et al. 2023b). GRMHD sim-

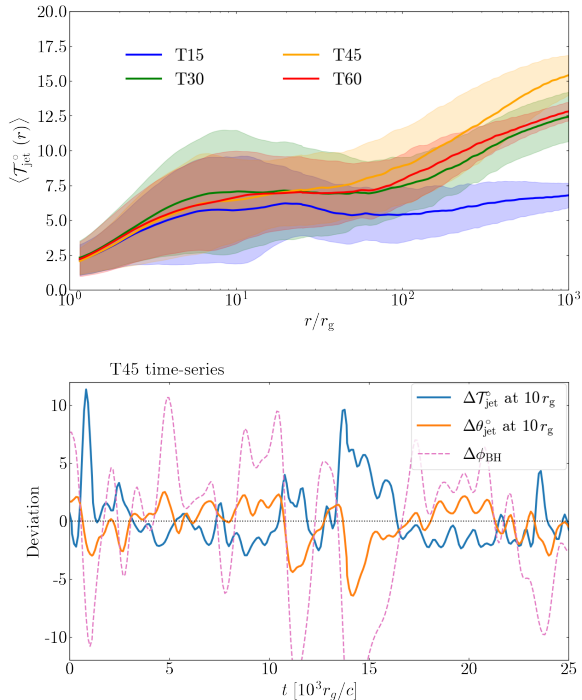


**Figure 9.** Despite alignment, jets wobble significantly due to magnetic flux eruptions and can appear to be precessing over periods of several years (for a  $10^9 M_{\odot}$  BH). (Top) We show radial profiles of the jet tilt angle with  $1\sigma$  standard deviation for the moderately misaligned MAD models T15–60. (Bottom) We find that deviations in the jet opening angle  $\theta_{\text{jet}}$  and orientation  $\mathcal{T}_{\text{jet}}$  are correlated and anti-correlated with the horizon magnetic flux  $\phi_{\text{BH}}$ . We track time-series curves of the deviations of the horizon magnetic flux and the jet tilt angle from their respective mean values for one model T45 over  $5 \times 10^4 r_g/c$ . The jet becomes wider ( $\theta_{\text{jet}}$  increases) as the MAD state develops ( $\phi_{\text{BH}}$  increases). Large excursions in  $\mathcal{T}_{\text{jet}}$  align with drops in  $\phi_{\text{BH}}$  caused by magnetic flux eruption events.

ulations that attempt to describe this particular BH accretion mode, such as the models in this work, are typically initialized with a rotating torus of gas with a disk height-to-radius ratio,  $h/r \approx 0.3 - 0.6$ , and a size  $r_{\text{disk}} \sim 50 - 1000 r_g$ , or more often depending on the amount of magnetic flux required for the specific problem. The tori in the initial conditions that result in weakly magnetized disks are typically small ( $\sim 50 r_g$  in size; e.g., Gammie et al. 2003; Porth et al. 2019), whereas magnetically arrested disks (MADs) require large-scale poloidal magnetic field loops and therefore, the initial tori often stretch out to  $1000 r_g$  (e.g., Chatterjee & Narayan 2022, see Tchekhovskoy 2015 for a discussion).

The initial torus develops MHD instabilities and gradually generates disk outflows, viscously spreads out over

time, and forms thick accretion flows ( $h/r \gtrsim 0.3$ ). The simulations in this work, along with models from Liska et al. (2018) and Chatterjee et al. (2020), undergo similar evolution but feature misaligned accretion disks. A misaligned disk initially behaves as a quasi-rigid body and undergoes LT precession before expanding radially and settling into a non-precessing warped disk (as seen in Fig. 1e,f in Liska et al. 2018 and Fig. 2e in Chatterjee et al. 2020). This is also why it is important to evolve tilted disks to runtimes long enough to develop a quasi-steady-state disk. We generally find simulation runtimes of  $t \approx 10^5 r_g/c$  to be enough for this purpose. The viscous expansion of the disk is crucial for achieving the quasi-steady-state warped disk as under-resolved disks continue to behave as rigid bodies and carry on precessing (see Fig. 1e of Liska et al. 2018, for comparisons between underresolved and resolved tilted disks). If the numerical resolution is insufficient to resolve the MRI in the outer disk, the disk will not be able to viscously expand, and hence precess at a constant rate.

Usually we see that disks develop a steady warped morphology when LT torques are significant (i.e., when the BH spin magnitude is large and/or there are strong poloidal magnetic fields in the vicinity of the BH). As we show in this work, misaligned MAD flows onto high spin prograde BHs are a notable exception as the jet torques the inner disk into alignment (which also means that there cannot be any substantial disk or jet precession). Overall we suggest that jets from resolved misaligned, geometrically-thick accretion disks *do not* exhibit LT precession (also see Nixon & King 2013). While this statement should hold true for highly sub-Eddington accretion flows where the inflow is geometrically-thick out to large distances, there is evidence from recent simulations that a magnetized, thick inner disk fed by an outer geometrically-thin disk also fails to precess substantially (Bollimpalli et al. 2023). Currently, disk precession in GRMHD simulations has only been demonstrated for highly misaligned (initial  $\mathcal{T}_{\text{disk}} = 65^\circ$ ), geometrically-thin ( $h/r \approx 0.03$ ) disks where the inner disk is able to tear off from the outer disk (Nixon et al. 2012; Liska et al. 2021, 2022, 2023a) and can precess over multiple orbits. Disk tearing could be a viable candidate for explaining X-ray quasi-periodic oscillations seen in the hard-intermediate state of XRBs (Musoke et al. 2023).

Lightcurve periodicities and precession-like wobbling are also seen in AGN jets: possible models involve orbital precession due to candidate binary black holes (e.g., for OJ287, Britzen et al. 2023) and LT precession. Further, the jet in M87 has a measurable transverse displacement with a quasi-periodicity of 8-10 years (Walker et al. 2018). If not LT precession, fluid instabilities such

as the Kelvin-Helmholtz instability (KHI) are invoked to partially explain jet wobbling and apparent precession, but there are also counter-arguments to this reasoning, chief of which is whether KHI can actually drive large-scale lateral motion. Other than KHI, collisions between the jet base and the disk wind can also drive oscillations in the jet orientation. Jets from MAD accretion flows (aligned or tilted) exhibit wobbling with  $1\sigma$  standard deviation of  $3 - 5^\circ$  in the jet tilt angle (Fig. 9 and Table 1). Displacements of even a few degrees may become substantial when the jet is viewed at certain inclination angles due to Doppler effects. Such oscillations in the jet base could then potentially explain quasi-periodic shifts in the radio core position of blazar jets (e.g., Weaver et al. 2022).

Other than jet-wind collisions, magnetic flux eruption events in MAD could lead to substantial lateral displacements in the jet base. Figure 9 (bottom) shows the deviation in jet tilt angle,  $\mathcal{T}_{\text{jet}}$ , (or orientation angle) and the jet opening angle,  $\theta_{\text{jet}}$ , at  $10 r_g$  and the normalized magnetic flux at the BH horizon,  $\phi_{\text{BH}}$ , from their mean values over a period of  $5 \times 10^4 r_g/c$  (or  $\approx 50$  years for M87). Eruption events, indicated by a sharp drop in  $\phi_{\text{BH}}$ , release cylindrical tubes of vertical magnetic fields that then interact with the accreting gas (e.g., Chatterjee & Narayan 2022), and can generate high energy flares (Chatterjee et al. 2021; Ripperda et al. 2022). Additionally, during eruption periods, while  $\theta_{\text{jet}}$  at  $10 r_g$  drops as well, there are no significant changes at larger scales. During the largest eruption events,  $\mathcal{T}_{\text{jet}}$  at  $10 r_g$  can change by nearly  $10^\circ$ , and the largest deviations in the jet orientation are spaced roughly  $10^4 r_g/c$  apart, approximately 10 years for M87, potentially providing an alternate origin for precession-like behavior in the jet base (see also Lalakos et al. 2023). Further, these lateral excursions drive waves through the jet-wind shear layer (Davelaar et al. 2023) that could develop into the large-scale flow patterns often seen in radio images of jets, manifesting in quasi-periodic position angle shifts (e.g., as seen in Cui et al. 2023). Simultaneous detections of bright flares (from X-rays to TeV energies) with observed lateral shifts in radio jets could verify whether magnetic flux eruptions could indeed be a viable alternative to orbital or LT precession for quasi-periodic jet motion in the sub-Eddington accretion regime.

Finally, we note that the time spacing between large magnetic eruption events can vary significantly and could be dependent on the geometrical thickness of the disk. Though we neglect the effects of radiative cooling, our simulations should be applicable for M87 ( $\dot{M} \approx 10^{-4} \dot{M}_{\text{Edd}}$ ) as the disk does not lose significant vertical pressure support due to radiative cooling and re-

mains geometrically-thick (Chatterjee et al. 2023; Liska et al. 2023b). We leave the exploration of the properties of magnetic flux eruptions for different misaligned disks to future work.

## 5. CONCLUSIONS

In this work, our goal is to deconstruct the evolution of highly magnetized accretion disks (“MADs”) whose angular momentum axis is misaligned relative to the black hole (BH) spin axis. For this, we simulate an extensive set of GRMHD simulations of disks with 7 different initial tilt angles, ranging from  $0^\circ$  and  $90^\circ$ , around a Kerr BH of spin parameter  $a = 0.9375$ . Additionally, we spot-check other spin values ( $a = -0.9375, \pm 0.5$ ) and consider other near-MAD magnetic setups. Table 1 provides a summary of all our models.

We summarize our results here:

1. Given enough magnetic flux supply and a rapidly spinning BH, geometrically-thick disks ( $h/r \sim 0.3$ ) tilted at  $\mathcal{T} \lesssim 60^\circ$  can be forced into magneto-spin alignment with the BH spin axis, out to  $r \lesssim 100 r_g$ .
2. Extremely misaligned MAD disks,  $\mathcal{T} \gtrsim 75^\circ$ , around rapidly spinning BHs exhibit intermittent jetted outbursts, separated by quiet periods of  $\Delta t \sim 5 \times 10^4 r_g/c$ . Interestingly, in the process of aligning the disk, these jets expel the disk’s magnetic flux out to 1000s of  $r_g$ , inadvertently choking their own flux supply. However, over time, some portion of the disk poloidal flux reaches the BH horizon again, reactivates the MAD state and the jets, and the cycle repeats again. This is the first demonstration of restarted jets in GRMHD simulations and could explain transient radio and X-ray activity (due to shocks via jet-disk interactions) in otherwise low-luminosity BH systems.
3. Magneto-spin alignment of the disk depends on both the magnitude of the magnetic flux on the BH horizon and the BH spin. Our models suggest that only highly spinning prograde BHs in the MAD state can produce jets powerful enough to magnetically align geometrically-thick accretion disks.
4. For jets that are unable to magneto-spin-align a tilted disk, the disk shows radial tilt oscillations. In this case, increasing the initial disk tilt angle results in lower horizon magnetic flux values and lower jet powers. The jet power also changes with both the spin and tilt angle as the MAD magnetic flux saturation value is different for different spins, similar to their aligned version (e.g., Tchekhovskoy

et al. 2012; Tchekhovskoy 2015; Narayan et al. 2022; Lowell et al. 2023).

5. Finally, combining the results from this work and previous literature for tilted thick disks, we find that the disk/jet does not undergo Lense-Thirring precession for highly sub-Eddington BH accretion flows ( $\dot{M} \ll 10^{-3}\dot{M}_{\text{Edd}}$ ). We suggest that the large jet wobbling amplitude seen during magnetic flux eruption events could provide an alternate mechanism for precession-like behavior in AGN jets (e.g., for M87; Walker et al. 2018; Cui et al. 2023), with an approximate time period of several years for a  $10^9 M_{\odot}$  BH.

#### ACKNOWLEDGEMENTS

We thank Ramesh Narayan, Yuri Kovalev and Vladislav Makeev for useful discussions on accretion and curved jets. KC was supported in part by grants

from the Gordon and Betty Moore Foundation and the John Templeton Foundation to the Black Hole Initiative at Harvard University, and by NSF award OISE-1743747. ML was supported by the John Harvard, ITC and NASA Hubble Fellowship Program fellowships. AT acknowledges support from the NSF AST-2009884 and NASA 80NSSC21K1746 grants. AT was supported by BSF grant 2020747 and NSF grants AST-2107839, AST-1815304, AST-1911080, AST-2206471, OAC-2031997. This research was enabled by support provided by a INCITE program award PHY129, using resources from the Oak Ridge Leadership Computing Facility, Summit, which is a US Department of Energy office of Science User Facility supported under contract DE-AC05-00OR22725, as well as Calcul Quebec (<http://www.calculquebec.ca>) and Compute Canada (<http://www.computecanada.ca>). This work has made use of NASA’s Astrophysics Data System (ADS).

#### REFERENCES

- Bardeen, J. M., & Petterson, J. A. 1975, *ApJL*, 195, L65, doi: [10.1086/181711](https://doi.org/10.1086/181711)
- Beck, R., Brandenburg, A., Moss, D., Shukurov, A., & Sokoloff, D. 1996, *ARA&A*, 34, 155, doi: [10.1146/annurev.astro.34.1.155](https://doi.org/10.1146/annurev.astro.34.1.155)
- Begelman, M. C., Scepi, N., & Dexter, J. 2022, *MNRAS*, 511, 2040, doi: [10.1093/mnras/stab3790](https://doi.org/10.1093/mnras/stab3790)
- Blandford, R., Meier, D., & Readhead, A. 2019, *ARA&A*, 57, 467, doi: [10.1146/annurev-astro-081817-051948](https://doi.org/10.1146/annurev-astro-081817-051948)
- Blandford, R. D., & Znajek, R. L. 1977, *MNRAS*, 179, 433
- Bollimpalli, D. A., Fragile, P. C., & Kluźniak, W. 2023, *MNRAS*, 520, L79, doi: [10.1093/mnrasl/slac155](https://doi.org/10.1093/mnrasl/slac155)
- Bondi, H., & Hoyle, F. 1944, *MNRAS*, 104, 273, doi: [10.1093/mnras/104.5.273](https://doi.org/10.1093/mnras/104.5.273)
- Brandenburg, A., & Subramanian, K. 2005, *PhR*, 417, 1, doi: [10.1016/j.physrep.2005.06.005](https://doi.org/10.1016/j.physrep.2005.06.005)
- Britzen, S., Zajaček, M., Gopal-Krishna, et al. 2023, *ApJ*, 951, 106, doi: [10.3847/1538-4357/acbbc](https://doi.org/10.3847/1538-4357/acbbc)
- Caprioli, D. 2015, *ApJL*, 811, L38, doi: [10.1088/2041-8205/811/2/L38](https://doi.org/10.1088/2041-8205/811/2/L38)
- Chatterjee, K., Liska, M., Tchekhovskoy, A., & Markoff, S. B. 2019, *MNRAS*, 490, 2200, doi: [10.1093/mnras/stz2626](https://doi.org/10.1093/mnras/stz2626)
- Chatterjee, K., & Narayan, R. 2022, *ApJ*, 941, 30, doi: [10.3847/1538-4357/ac9d97](https://doi.org/10.3847/1538-4357/ac9d97)
- Chatterjee, K., Younsi, Z., Liska, M., et al. 2020, *MNRAS*, 499, 362, doi: [10.1093/mnras/staa2718](https://doi.org/10.1093/mnras/staa2718)
- Chatterjee, K., Markoff, S., Neilsen, J., et al. 2021, *MNRAS*, 507, 5281, doi: [10.1093/mnras/stab2466](https://doi.org/10.1093/mnras/stab2466)
- Chatterjee, K., Chael, A., Tiede, P., et al. 2023, *Galaxies*, 11, 38, doi: [10.3390/galaxies11020038](https://doi.org/10.3390/galaxies11020038)
- Crumley, P., Caprioli, D., Markoff, S., & Spitkovsky, A. 2019, *MNRAS*, 485, 5105, doi: [10.1093/mnras/stz232](https://doi.org/10.1093/mnras/stz232)
- Cui, Y., Hada, K., Kawashima, T., et al. 2023, *Nature*, 621, 711, doi: [10.1038/s41586-023-06479-6](https://doi.org/10.1038/s41586-023-06479-6)
- Davelaar, J., Ripperda, B., Sironi, L., et al. 2023, *arXiv e-prints*, arXiv:2309.07963, doi: [10.48550/arXiv.2309.07963](https://doi.org/10.48550/arXiv.2309.07963)
- Dexter, J., & Fragile, P. C. 2013, *MNRAS*, 432, 2252, doi: [10.1093/mnras/stt583](https://doi.org/10.1093/mnras/stt583)
- Edgar, R. 2004, *NewAR*, 48, 843, doi: [10.1016/j.newar.2004.06.001](https://doi.org/10.1016/j.newar.2004.06.001)
- Evans, P. A., Nixon, C. J., Campana, S., et al. 2023, *Nature Astronomy*, doi: [10.1038/s41550-023-02073-y](https://doi.org/10.1038/s41550-023-02073-y)
- Event Horizon Telescope Collaboration, Akiyama, K., Alberdi, A., et al. 2019, *ApJL*, 875, L5, doi: [10.3847/2041-8213/ab0f43](https://doi.org/10.3847/2041-8213/ab0f43)
- . 2022, *ApJL*, 930, L16, doi: [10.3847/2041-8213/ac6672](https://doi.org/10.3847/2041-8213/ac6672)
- Fabian, A. C. 2012, *Annual Review of Astronomy and Astrophysics*, 50, 455, doi: [10.1146/annurev-astro-081811-125521](https://doi.org/10.1146/annurev-astro-081811-125521)
- Fender, R. P., Belloni, T. M., & Gallo, E. 2004, *MNRAS*, 355, 1105, doi: [10.1111/j.1365-2966.2004.08384.x](https://doi.org/10.1111/j.1365-2966.2004.08384.x)
- Ferrière, K. 2020, *Plasma Physics and Controlled Fusion*, 62, 014014, doi: [10.1088/1361-6587/ab49eb](https://doi.org/10.1088/1361-6587/ab49eb)
- Fishbone, L. G., & Moncrief, V. 1976, *ApJ*, 207, 962, doi: [10.1086/154565](https://doi.org/10.1086/154565)

- Fragile, P. C., Blaes, O. M., Anninos, P., & Salmonson, J. D. 2007, *ApJ*, 668, 417, doi: [10.1086/521092](https://doi.org/10.1086/521092)
- Gammie, C. F., McKinney, J. C., & Tóth, G. 2003, *ApJ*, 589, 444, doi: [10.1086/374594](https://doi.org/10.1086/374594)
- Guolo, M., Pasham, D. R., Zajaček, M., et al. 2023, arXiv e-prints, arXiv:2309.03011, doi: [10.48550/arXiv.2309.03011](https://doi.org/10.48550/arXiv.2309.03011)
- Harrison, C. M., Costa, T., Tadhunter, C. N., et al. 2018, *Nature Astronomy*, 2, 198, doi: [10.1038/s41550-018-0403-6](https://doi.org/10.1038/s41550-018-0403-6)
- Haverkorn, M., & Spangler, S. R. 2013, *SSRv*, 178, 483, doi: [10.1007/s11214-013-0014-6](https://doi.org/10.1007/s11214-013-0014-6)
- Hoyle, F., & Lyttleton, R. A. 1939, *Proceedings of the Cambridge Philosophical Society*, 35, 405, doi: [10.1017/S0305004100021150](https://doi.org/10.1017/S0305004100021150)
- Ingram, A. R., & Motta, S. E. 2019, *NewAR*, 85, 101524, doi: [10.1016/j.newar.2020.101524](https://doi.org/10.1016/j.newar.2020.101524)
- Kaaz, N., Liska, M. T. P., Jacquemin-Ide, J., et al. 2023, *ApJ*, 955, 72, doi: [10.3847/1538-4357/ace051](https://doi.org/10.3847/1538-4357/ace051)
- Lalakos, A., Tchekhovskoy, A., Bromberg, O., et al. 2023, arXiv e-prints, arXiv:2310.11487, doi: [10.48550/arXiv.2310.11487](https://doi.org/10.48550/arXiv.2310.11487)
- Lalakos, A., Gottlieb, O., Kaaz, N., et al. 2022, arXiv e-prints, arXiv:2202.08281, <https://arxiv.org/abs/2202.08281>
- Lense, J., & Thirring, H. 1918, *Physikalische Zeitschrift*, 19
- Liska, M., Hesp, C., Tchekhovskoy, A., et al. 2018, *MNRAS*, 474, L81, doi: [10.1093/mnrasl/slx174](https://doi.org/10.1093/mnrasl/slx174)
- . 2023a, *NewA*, 101, 102012, doi: [10.1016/j.newast.2023.102012](https://doi.org/10.1016/j.newast.2023.102012)
- . 2021, *MNRAS*, 507, 983, doi: [10.1093/mnras/staa099](https://doi.org/10.1093/mnras/staa099)
- Liska, M., Tchekhovskoy, A., Ingram, A., & van der Klis, M. 2019, *MNRAS*, 487, 550, doi: [10.1093/mnras/stz834](https://doi.org/10.1093/mnras/stz834)
- Liska, M. T. P., Kaaz, N., Chatterjee, K., Emami, R., & Musoke, G. 2023b, arXiv e-prints, arXiv:2309.15926, doi: [10.48550/arXiv.2309.15926](https://doi.org/10.48550/arXiv.2309.15926)
- Liska, M. T. P., Chatterjee, K., Issa, D., et al. 2022, *ApJS*, 263, 26, doi: [10.3847/1538-4365/ac9966](https://doi.org/10.3847/1538-4365/ac9966)
- Lowell, B., Jacquemin-Ide, J., Tchekhovskoy, A., & Duncan, A. 2023, arXiv e-prints, arXiv:2302.01351, doi: [10.48550/arXiv.2302.01351](https://doi.org/10.48550/arXiv.2302.01351)
- Matthews, J. H., Bell, A. R., Blundell, K. M., & Araudo, A. T. 2018, *MNRAS*, 479, L76, doi: [10.1093/mnrasl/sly099](https://doi.org/10.1093/mnrasl/sly099)
- McKinney, J. C., & Gammie, C. F. 2004, *ApJ*, 611, 977, doi: [10.1086/422244](https://doi.org/10.1086/422244)
- McKinney, J. C., Tchekhovskoy, A., & Blandford, R. D. 2012, *MNRAS*, 423, 3083, doi: [10.1111/j.1365-2966.2012.21074.x](https://doi.org/10.1111/j.1365-2966.2012.21074.x)
- . 2013, *Science*, 339, 49, doi: [10.1126/science.1230811](https://doi.org/10.1126/science.1230811)
- Musoke, G., Liska, M., Porth, O., van der Klis, M., & Ingram, A. 2023, *MNRAS*, 518, 1656, doi: [10.1093/mnras/stac2754](https://doi.org/10.1093/mnras/stac2754)
- Narayan, R., Chael, A., Chatterjee, K., Ricarte, A., & Curd, B. 2022, *MNRAS*, 511, 3795, doi: [10.1093/mnras/stac285](https://doi.org/10.1093/mnras/stac285)
- Narayan, R., Igumenshchev, I. V., & Abramowicz, M. A. 2003, *PASJ*, 55, L69, doi: [10.1093/pasj/55.6.L69](https://doi.org/10.1093/pasj/55.6.L69)
- Narayan, R., Sądowski, A., Penna, R. F., & Kulkarni, A. K. 2012, *MNRAS*, 426, 3241, doi: [10.1111/j.1365-2966.2012.22002.x](https://doi.org/10.1111/j.1365-2966.2012.22002.x)
- Nixon, C., & King, A. 2013, *ApJL*, 765, L7, doi: [10.1088/2041-8205/765/1/L7](https://doi.org/10.1088/2041-8205/765/1/L7)
- Nixon, C., King, A., Price, D., & Frank, J. 2012, *ApJL*, 757, L24, doi: [10.1088/2041-8205/757/2/L24](https://doi.org/10.1088/2041-8205/757/2/L24)
- Papaloizou, J. C. B., & Lin, D. N. C. 1995, *ARA&A*, 33, 505, doi: [10.1146/annurev.aa.33.090195.002445](https://doi.org/10.1146/annurev.aa.33.090195.002445)
- Polko, P., & McKinney, J. C. 2017, *MNRAS*, 464, 2660, doi: [10.1093/mnras/stw1875](https://doi.org/10.1093/mnras/stw1875)
- Porth, O., Chatterjee, K., Narayan, R., et al. 2019, *ApJS*, 243, 26, doi: [10.3847/1538-4365/ab29fd](https://doi.org/10.3847/1538-4365/ab29fd)
- Ressler, S. M., Quataert, E., White, C. J., & Blaes, O. 2021, *MNRAS*, 504, 6076, doi: [10.1093/mnras/stab311](https://doi.org/10.1093/mnras/stab311)
- Ressler, S. M., Tchekhovskoy, A., Quataert, E., & Gammie, C. F. 2017, *MNRAS*, 467, 3604, doi: [10.1093/mnras/stx364](https://doi.org/10.1093/mnras/stx364)
- Ressler, S. M., White, C. J., Quataert, E., & Stone, J. M. 2020, *ApJL*, 896, L6, doi: [10.3847/2041-8213/ab9532](https://doi.org/10.3847/2041-8213/ab9532)
- Reynolds, C. S. 2021, *ARA&A*, 59, 117, doi: [10.1146/annurev-astro-112420-035022](https://doi.org/10.1146/annurev-astro-112420-035022)
- Ricarte, A., Narayan, R., & Curd, B. 2023, *ApJL*, 954, L22, doi: [10.3847/2041-8213/aceda5](https://doi.org/10.3847/2041-8213/aceda5)
- Ripperda, B., Liska, M., Chatterjee, K., et al. 2022, *ApJL*, 924, L32, doi: [10.3847/2041-8213/ac46a1](https://doi.org/10.3847/2041-8213/ac46a1)
- Sironi, L., Petropoulou, M., & Giannios, D. 2015, *MNRAS*, 450, 183, doi: [10.1093/mnras/stv641](https://doi.org/10.1093/mnras/stv641)
- Tchekhovskoy, A. 2015, in *ASSL*, Vol. 414, *The Formation and Disruption of Black Hole Jets*, ed. I. Contopoulos, D. Gabuzda, & N. Kylafis, 45, doi: [10.1007/978-3-319-10356-3\\_3](https://doi.org/10.1007/978-3-319-10356-3_3)
- Tchekhovskoy, A., McKinney, J. C., & Narayan, R. 2012, in *Journal of Physics Conference Series*, Vol. 372, *Journal of Physics Conference Series*, 012040, doi: [10.1088/1742-6596/372/1/012040](https://doi.org/10.1088/1742-6596/372/1/012040)
- Tchekhovskoy, A., Narayan, R., & McKinney, J. C. 2010, *ApJ*, 711, 50, doi: [10.1088/0004-637X/711/1/50](https://doi.org/10.1088/0004-637X/711/1/50)
- . 2011, *MNRAS*, 418, L79, doi: [10.1111/j.1745-3933.2011.01147.x](https://doi.org/10.1111/j.1745-3933.2011.01147.x)
- Ubertosi, F., Gitti, M., Brighenti, F., et al. 2021, *ApJL*, 923, L25, doi: [10.3847/2041-8213/ac374c](https://doi.org/10.3847/2041-8213/ac374c)

- Volonteri, M., Madau, P., Quataert, E., & Rees, M. J. 2005, ApJ, 620, 69, doi: [10.1086/426858](https://doi.org/10.1086/426858)
- Walker, R. C., Hardee, P. E., Davies, F. B., Ly, C., & Junor, W. 2018, ApJ, 855, 128, doi: [10.3847/1538-4357/aaafcc](https://doi.org/10.3847/1538-4357/aaafcc)
- Weaver, Z. R., Jorstad, S. G., Marscher, A. P., et al. 2022, ApJS, 260, 12, doi: [10.3847/1538-4365/ac589c](https://doi.org/10.3847/1538-4365/ac589c)
- White, C. J., Dexter, J., Blaes, O., & Quataert, E. 2020, ApJ, 894, 14, doi: [10.3847/1538-4357/ab8463](https://doi.org/10.3847/1538-4357/ab8463)
- White, C. J., Quataert, E., & Blaes, O. 2019, ApJ, 878, 51, doi: [10.3847/1538-4357/ab089e](https://doi.org/10.3847/1538-4357/ab089e)

## 6. APPENDIX

6.1. *Does misalignment depend on accretion history?*

In our fiducial model set, we initialize the BH with a spin vector along the  $z$ -axis and rotate the disk by an initial misalignment angle. To test the robustness of our results, we perform 3 moderate-resolution ( $580 \times 192 \times 384$ ) simulations where we rotate the BH spin vector instead of the disk. We dub these models as TxBH where ‘x’ ( $\equiv 0, 60$  and  $90$ ) is the BH misalignment angle with respect to the  $z$ -axis in degrees. Additionally we follow the approach of McKinney et al. (2013) and only change the BH spin orientation *after* the initially non-tilted BH-disk (model TOBH) system reaches the MAD state at  $t = 2.5 \times 10^4 r_g/c$ . Such an approach will also test whether our results from the fiducial simulations is robust against accretion history, i.e., does alignment depend on whether the initial flow was in the magnetically arrested state?

Figure 10 shows that the tilted BH models behave similar to the “tilted disk” simulations over all: (i) the non-tilted TOBH continues to show powerful jets; (ii) the  $60^\circ$  tilt model, T60BH considerably aligns with the BH midplane and displays prominent jets until  $t \sim 4.5 \times 10^4 r_g/c$ . As we see from the disk magnetic flux plot of T60BH, around the same time as the jet ceases, there is a significant loss of magnetic flux in the disk, indicating a jet-disk collision; (iii) The  $90^\circ$  model, T90BH does not really exhibit any prominent jets. However when we decreased the plasma- $\beta$  by a factor of 10 in model T90BHb, we see similar jet-disk collisions as seen in model T90. While more rigorous studies are required, our results seem to indicate that accretion history does not matter for alignment when the magnetic flux supply is large. However, if the flow is marginally MAD, there is a possibility that the flow becomes non-MAD upon introducing misalignment.

6.2. *Grid checking: the Schwarzschild case*

Here we check how well our grid performs as we tilt our disk from the equatorial midplane at  $\theta = \pi/2$  to the pole at  $\theta = 0$  in the case of a spin-zero BH. Since the spin is zero, ideally these two disks should evolve similarly barring stochastic turbulence. Figure 11 shows that all of our disk properties match remarkably well between the two disks, especially the radial profiles of the Maxwell, Reynolds and the total effective  $\alpha$  viscosities, providing confidence that our grid setup resolves the turbulence sufficiently well, and the polar axis is properly transmissive.

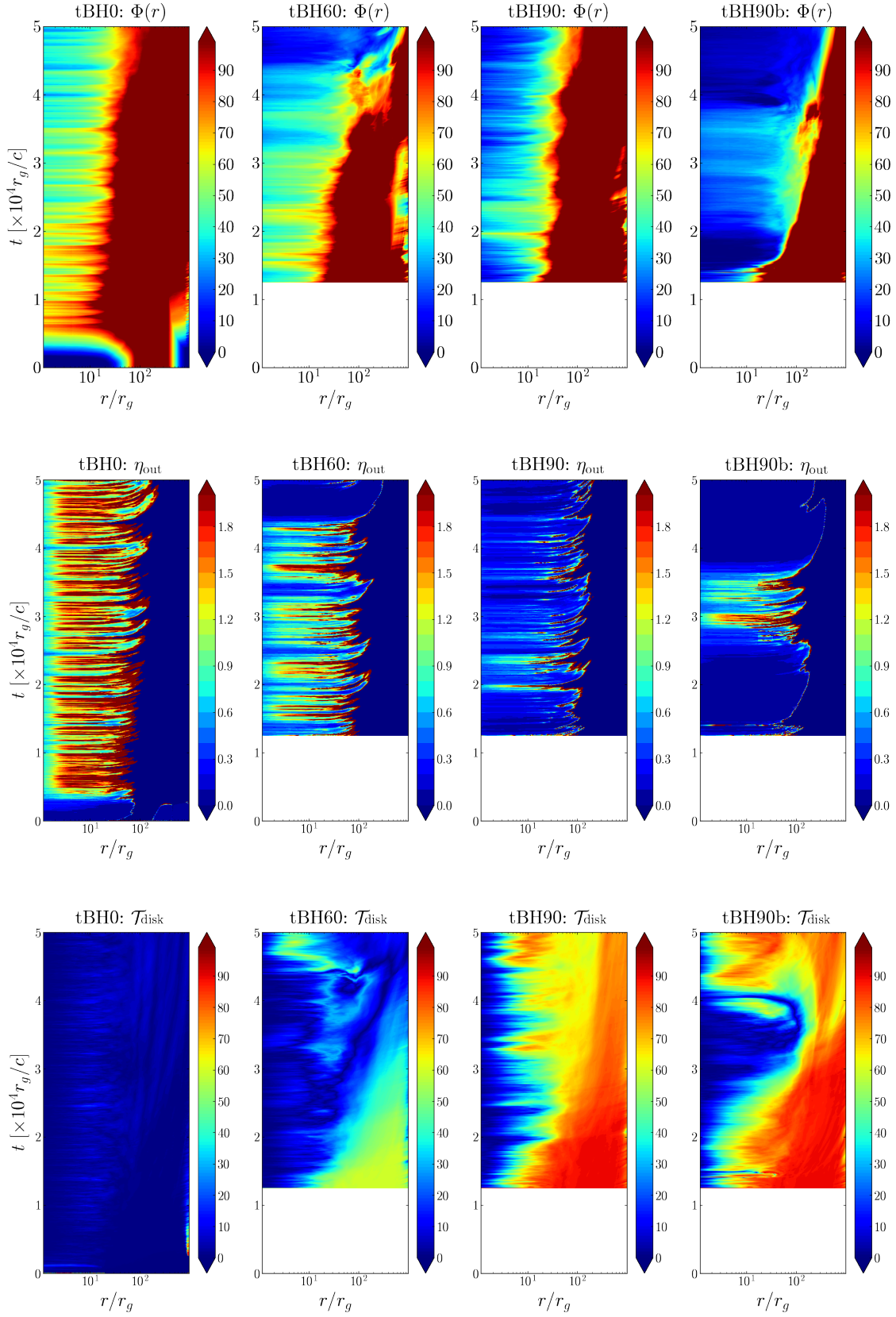


**Figure 10.** Space-time plots (similar to Fig. 5) of tilted black hole simulations, where instead of tilting the disk, we tilt the BH spin axis after the inner flow attains the MAD state.

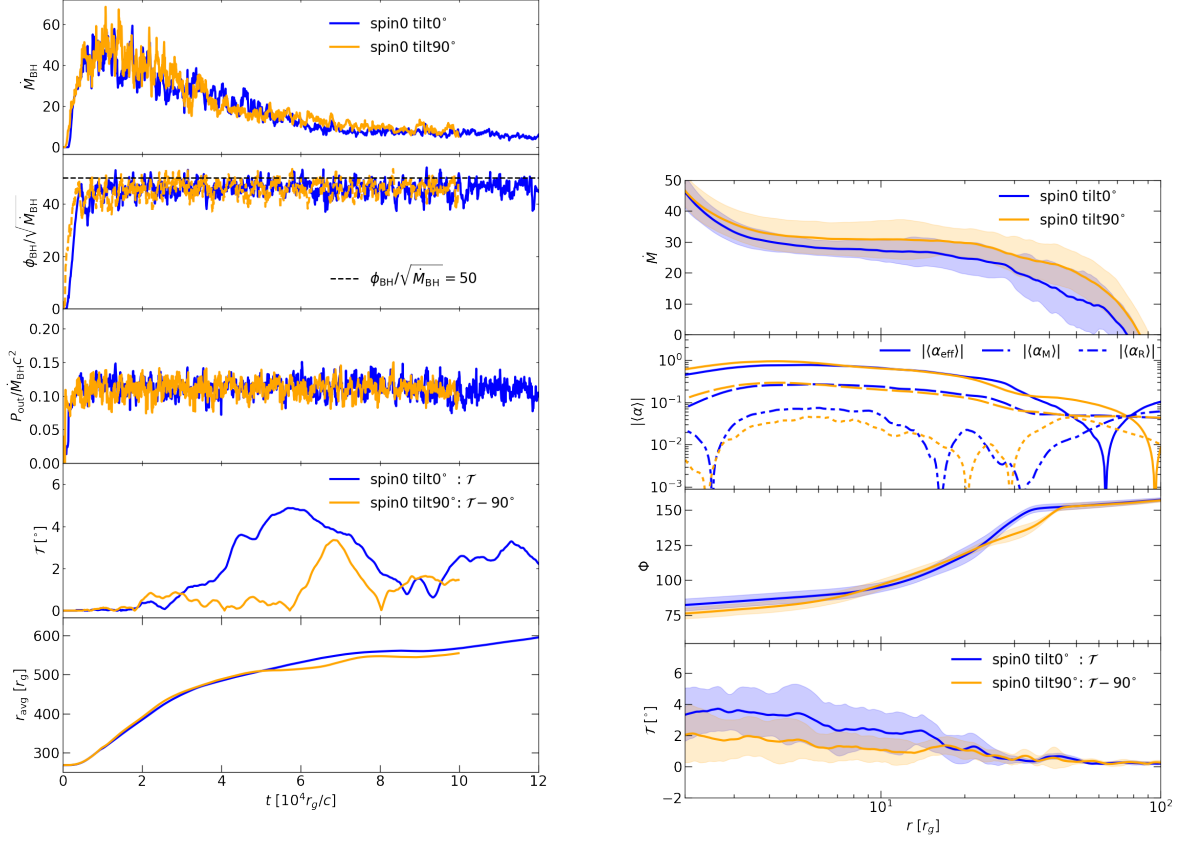


**Figure 11.** A comparison between a disk aligned to the polar grid midplane  $\theta = \pi/2$  and a disk aligned with the polar axis  $\theta = 0$  for a Schwarzschild BH. We look at multiple time and radial plots of disk properties and find that our grid setup behaves well when the disk is tilted.